Available online at
https://journal.uitm.edu.my/ojs/index.php/MJCET

e-ISSN: 2682-8588

Malaysian Journal of Chemical Engineering & Technology 7(2) 2024, 159–186

Malaysian Journal of Chemical Engineering and Technology

Quantitative accident analysis on two different bioethanol production plant

Muhammad Saber Khairunnizam[1], Mohd Aizad Ahmad[2*], Zulkifli Abdul Rashid[3], Nur Adlina Azhari[4]

[1,2,3,4]*School of Chemical Engineering, College of Engineering, Universiti Teknologi MARA, 40450 Shah Alam, Selangor, Malaysia*

ARTICLE INFO

Article history:
Received 1 July 2024
Revised 23 October 2024
Accepted 23 October 2024
Online first
Published 31 October 2024

Keywords:
Bioethanol Production
Chemical Release
Fatalities
Incident Outcome Cases
Quantitative Accident Analysis

DOI:
10.24191/mjcet.v7i2.1863

ABSTRACT

The purpose of this study is to examine the expected percentage of fatalities caused by three significant equipment mishaps at a recently built facility in Selangor, Malaysia. This study investigated the possibility of (1) various events occurring in terms of toxicity, thermal radiation, and overpressure, and (2) the percentage of fatalities resulting from the release of chemical mixtures from two ethanol plants: the reference plant (Plant 1) and Plant 2. The major equipment includes a combustor reactor operating at 700 °C and 1 bar for both Plants 1 and 2, a gasification reactor operating at 700 °C (Plant 1) and 900 °C (Plant 2) at 20 bar, and a bioreactor operating at 37 °C and 1 bar for both Plants 1 and 2. To model the process and determine the mass density, mass fraction, and volume fraction of the mixture, Aspen Plus software was utilized. ALOHA and MARPLOT software were used to compute the quantity of toxicity, heat radiation, overpressure, and the affected area. The main equipment comprises a combination of carbon dioxide, carbon monoxide, hydrogen, ethanol, ethanoic acid, and water, with water considered non-harmful. The release of a chemical mixture was postulated and simulated using three-hole size scenarios: 10 mm, 25 mm, and 160 mm. The findings indicated that Plant 2 experienced the highest percentage of fatalities, 86.77%, resulting from the ethanol fireball incident during nighttime through a 25 mm leak.

1. INTRODUCTION

In this current age, global energy demand keeps rising and environmental concerns are being faced. The world must not be dependent on coal, crude oil, and natural gas as its main source of energy for further development as it is a non- renewable source and produces harmful pollutants. To prevent the use of non-renewable sources from depleting due to rising global energy demands, several researchers have proposed the use of biomass as a raw material that can be converted into energy rather than letting it go to waste.

[2*]Corresponding author. *E-mail address*: mohdaizad@uitm.edu.my
https://doi.org/10.24191/mjcet.v7i2.1863

Thus, attempts have been made to develop different technologies in the past few years to utilize biomass in different applications. One of them is to use biomass as a sustainable feedstock for renewable ethanol (Pardo-Planas et al., 2017).

Currently, three main process routes that effectively convert biomass into ethanol, that is, biochemical process, thermochemical process, and hybrid process (Michailos et al., 2017). The first one, the biochemical process, is divided into two main steps where the first step is the hydrolysis of the biomass to further break down the physicochemical structure of the material and release sugars which the sugar will be used in yeast fermentation to produce ethanol in step two. This is the most researched process because of its similarity with the existing production technology of ethanol and the anticipated lower capital cost (Liguori et al., 2016). But it comes with a main disadvantage, for this route, the lignin cannot be decomposed into a usable sugar during pre-treatment for the fermentation process rendering it useless for ethanol production. The second main process route is the thermochemical route where it transforms the biomass into syngas via gasification followed by mixed alcohol catalytic synthesis, but the drawback of this route is that it requires a high amount of energy and has low ethanol selectivity (Fang et al., 2009). The third main process route is the hybrid process which is a combination of gasification and fermentation. The biomass is first gasified then the syngas produced from gasification are fermented by acetogenic bacteria to produce ethanol (Michailos et al., 2017). The hybrid process has several advantages including higher yields, higher reaction specificity, lower energy demands, syngas composition versatility and higher resistance to impurities (Acharya et al., 2014).

For this production of ethanol, a hybrid process was used where biomass undergoes several reactions forming syngas (Michailos et al., 2017). The reactions to produce syngas consist of twelve equations containing heterogeneous and homogenous reactions. Among all the heterogeneous reactions, biomass devolatilization (R1) is the primary reaction forming gas, tar, and char, while Boudouard (R3) and carbon steam (R4) reactions are the main reactions between the solid char and gasifying agents of CO_2 and H_2O where the three reactions mentioned are all endothermic and can be favoured at higher temperature (Y. Zhang et al., 2020). Carbon gasification with O_2 (R2) and carbon methanation (R5) with hydrogen are exothermic reaction reactions that can provide some heat to drive the endothermic reactions (Y. Zhang et al., 2020). The homogeneous reactions, mainly involve reactions between the primary gaseous products and the gasifying agents (Y. Zhang et al., 2020). All the reactions with oxygen (R7 - R10) are exothermic, thus, providing the energy source for all the endothermic reactions, such as the steam reforming (R12) and dry reforming (R13) of methane (Y. Zhang et al., 2020). The methane combustion reaction (R10) releases large quantities of energy (up to 803 kJ/mol) (Y. Zhang et al., 2020). The water-gas shift reaction (R11) is of great importance when using steam as a gasifying medium to adjust the H_2 and CO ratio of the syngas (Y. Zhang et al., 2020).

Heterogeneous Reactions:

R1: CxHyOz (biomass) + heat → gas + tar + solid C (devolatilization) $\Delta H250°C$ = endothermic (1)

R2: $C + 0.5O_2 \rightarrow CO$ (carbon gasification) $\Delta H250°C = -111$ kJ/mol (2)

R3: $C + CO_2 \rightarrow 2CO$ (Boudard reaction) $\Delta H250°C = +172$ kJ/mol (3)

R4: $C + H_2O \rightarrow CO + H_2$ (carbon steam gasification) $\Delta H250°C = +131$ kJ/mol (4)

R5: $C + 2H_2 \rightarrow CH_4$ (hydrogasification) $\Delta H250°C = -75$ kJ/mol (5)

https://doi.org/10.24191/mjcet.v7i2.1863

Homogeneous Reactions:

R6: CnHmOp (tar) + heat → gas + solid C (decomposition) ΔH250°C = endothermic (6)

R7: $CO + 0.5O_2 \rightarrow CO_2$ (CO combustion) ΔH250°C = -283 kJ/mol (7)

R8: $H_2 + 0.5O2 \rightarrow H_2O$ (H2 combustion) ΔH250°C = -242 kJ/mol (8)

R9: $CH_4 + 0.5O_2 \rightarrow CO + 2H_2$ (CH_4 gasification) ΔH250°C = -36 kJ/mol (9)

R10: $CH_4 + 2O_2 \rightarrow CO_2 + 2H_2O$ (CH_4 combustion) ΔH250°C = -803 kJ/mol (10)

R11: $CO + H_2O \rightarrow CO_2 + H_2$ (water-gas shift) ΔH250°C = -41 kJ/mol (11)

R12: $CH_4 + H_2O \rightarrow CO + 3H_2$ (steam reforming) ΔH250°C = +206 kJ/mol (12)

R13: $CH_4 + CO_2 \rightarrow 2CO + 2H_2$ (dry reforming) ΔH250°C = +247 kJ/mol (13)

The syngas produced in an oxygen-blown circulated fluidized bed (CFB) reactor operating at 700 °C and 20 bar and then was used for fermentation to form ethanol as the main product and acetic acid as the by-product (Michailos et al., 2017). The syngas is then cooled by flowing through a series of heat exchangers until a temperature of 37 °C is reached before feeding it into a bioreactor for the fermentation process to avoid harming the bacterium. The reaction takes place in a continuously stirred tank bioreactor with operating conditions of temperature equal to 37 °C and pressure of 1 bar which consists of four equations catalysed by *bacterium C. ljungdahlii* (Michailos et al., 2017). Carbon monoxide from the syngas reacts with water to form ethanol, acetic acid, and carbon monoxide (R14 & R16) while carbon dioxide reacts with hydrogen to form ethanol, acetic acid and water (R15 & R17) (Michailos et al., 2017).

R14: $6CO + 3H_2O \rightarrow CH_3CH_2OH + 4CO_2$ (14)

R15: $2CO_2 + 6H_2 \rightarrow CH_3CH_2OH + 3H_2O$ (15)

R16: $4CO + 2H_2O \rightarrow CH_3COOH + 2CO_2$ (16)

R17: $2CO_2 + 4H_2 \rightarrow CH_3COOH + 2H_2O$ (17)

The combination of the thermochemical process and the biochemical process yielded 24% of ethanol with a conversion rate of 50% to 70% compared to another process such as the thermochemical process alone or the biochemical process along with lower energy consumption (Michailos et al., 2017). The combined process uses a pressure of up to 20 bar with operating temperatures ranging from 700 °C up to 1000 °C to achieve the mentioned yield and conversion rate (Michailos et al., 2017).

Because of its high operating temperature, the process is prone to a condition called thermal stress, which is inherently unsafe and poses greater risk compared to a biochemical process where the operating temperature is much lower (Heikkilä & Valtion, 1999). The high temperature paired with high-pressure operating conditions could lead to a higher probability of chemical leakages (Srinivasan & Nhan, 2008). Meanwhile, increased reaction enthalpy increases the likelihood of an explosion (Heikkilä, 1999). As a result, methods for producing ethanol using rice straw via combined thermochemical and biochemical

https://doi.org/10.24191/mjcet.v7i2.1863

necessitate risk evaluation and identification. The risk evaluation and identification can be done using the Consequence Analysis (CA) method (Ahmad et al., 2022). The Consequence Analysis (CA) established method can be divided into three procedures: (i) identifying and categorizing the installation and system that must be assessed; (ii) identifying hazardous substance and accident scenarios; and (iii) estimating the consequences scenario related to fatalities or injuries and equipment/building damage. To anticipate the impacts of concentrated chemicals discharged in terms of toxicity, heat radiation from a fire occurrence, and overpressure from an explosion scenario, consequence models are utilized. Consequence model comprise of toxic and dispersion model to calculate impact on toxicity, thermal radiation model calculate impact on fire while overpressure model estimate impact on explosion scenario (Casal, 2018a).

The purpose of this paper is to study the impact of carbon monoxide-carbon dioxide-hydrogen-ethanol-acetic acid-water (CO-CO_2-H_2-$EtOH$-CH_3COOH- H_2O) mixture release from two ethanol production plant, which are reference plant or plant 1 and plant 2, in terms of estimated fatalities percentage covering three different major equipment using CA method. These incidents covered the continuous emission of tiny and medium leaks with diameters of 10 mm and 25 mm. While the immediate release is represented by a 160 mm diameter leaking. The events that occur as a result of these release scenarios are determined by chemical properties, as only toxic chemicals such as carbon monoxide and carbon dioxide cause toxicity. For chemicals with toxic and flammable characteristics such as ethanol, acetic acid, and hydrogen, the release of the mentioned chemical could cause toxicity, jet fire, flash fire, pool fire, boiling liquid expanding vapour explosion (BLEVE) and vapor cloud explosion (VCE) effect. These effects are assessed in terms of fatalities percentage for different major equipment used in the production of ethanol, size of leakage of the major equipment, chemicals, and consequence events.

2. METHODOLOGY

This study was conducted to assess the possibility of establishing and operating a bioethanol production plant near a few rice mill factories to exploit large quantities of biomass being produced at the rice mill that will eventually be disposed of as industry waste. The plant had been suggested to be built in the area of Sekinchan, Selangor. Two plants, which are reference plant or plant 1 and plant 2 with different stream conditions entering and exiting the combustor reactor, gasification reactor, and bioreactor were simulated using Aspen Plus software version V12. The fatality assessments for the two plants are based on three similar major equipment which are the pyrolysis or combustor reactor (R-101), gasifier (R-102), and bioreactor (R-103) with the largest volume fraction of pure chemical component being H_2, CO, and C_2H_5OH, respectively. The main difference of plant 1 and plant 2 is the operating temperature for gasifier, where plant 1 operates at 700 °C, while plant 2 operating temperature is 900 °C. The operating temperature, pressure and reactor volume for combustor and bioreactor are similar for both plant 1 and plant 2.

2.1 Process condition of reference plant or plant 1

The condition for the reference plant or plant 1 for the combustor or pyrolysis reactor is operating at a temperature of 700 °C with pressure of 1 bar and reactor volume of 47.5 m^3, where the biomass was decomposed into pure elemental composition (Pardo- Planas et al., 2017). For the gasification reactor, it operates at a temperature of 700 °C, pressure of 20 bar and 43 m^3 reactor size to produce a syngas with mixture mainly composed of CO and H_2 with some CO_2 (Pardo-Planas et al., 2017). The bioreactor, which volume of 30 m^3, operates at 37 °C and at a pressure of 1 bar to produce bioethanol with side products of acetic acid and water (Pardo-Planas et al., 2017). The process flow can be seen in Figure A1, and the process condition of the plant can be seen in Table B1.

https://doi.org/10.24191/mjcet.v7i2.1863

2.2 Process condition of plant 2

To produce ethanol in this plant 2, gasification of rice straw and fermentation of syngas process was employed. The raw material is rice straw that had been bought from the nearest rice mill where paddy has been harvested to produce rice straw and rice. The rice straw is first fed into a combustor reactor at a rate of 50,000 kg/hr forming gas, tar, and char with the operating conditions at a temperature of 700 °C, at a pressure of 1 bar and volume of 47.5 m^3 as in reaction R1 and R6 (Griffin & Schultz, 2012). The product from the combustion is then fed into a gasifier with excess oxygen to form syngas comprised of CO, CO_2, H_2, and H_2O (CH_4 was neglected since the amount produced is very small) with compositions of 24%, 12.6%, 1.2% and 4.6%, respectively, using Aspen Plus Version 12 with the operating condition at a temperature of 900 °C, a pressure of 20 bars and reactor size of 43 m^3 as in reaction R2 to R5.

For the fermentation process, the cooled-down syngas was fed into a bioreactor with excess air forming ethanol, acetic acid, water, and carbon dioxide as in reaction R14 to R17 with the bioreactor with reactor volume of 30 m^3, operating at a temperature of 37 °C and a pressure of 1 bar. The product leaving the reactor is then fed into a separating vessel to separate the unreacted gas (carbon monoxide, carbon dioxide, and hydrogen) from the product (ethanol, acetic acid, and water). The product was then purified using distillation columns until a targeted purity of 95% pure ethanol was achieved. Figure A2 shows the process flow of the plant. Table B2 summarizes the process condition of the plant.

2.3 Process plant location

This plant is suggested to be built in Sekinchan, Selangor near paddy fields and rice mills. The location was chosen because the biomass being produced by the rice mill was used as raw material. The location is illustrated in Fig. 1. The meteorological data for the Sekinchan area are assessed using a weather station at Tanjung Karang, a small district of Sekinchan. Table B3 shows the meteorological data used to simulate events occurring for all case studies.

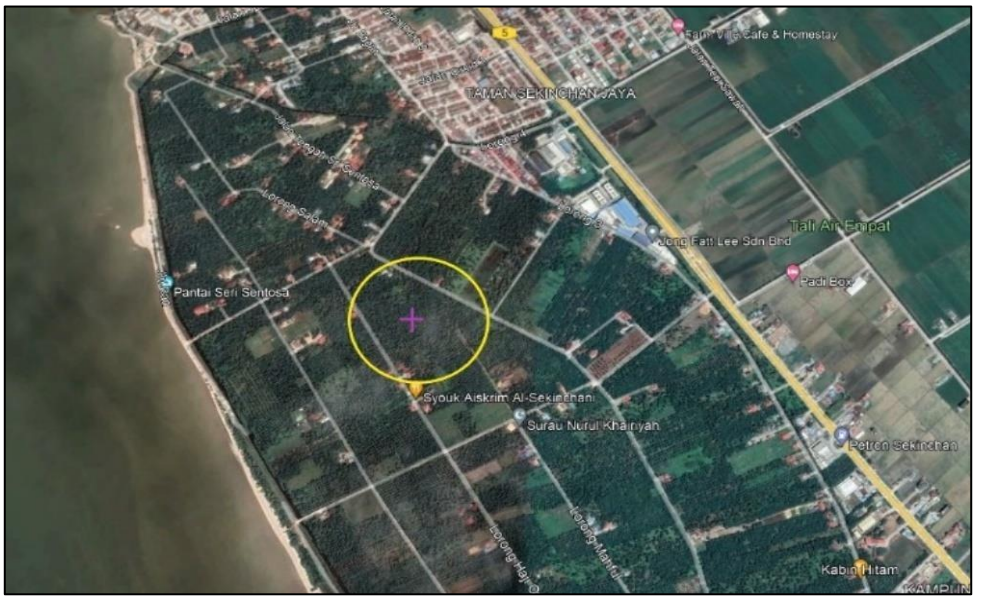

Fig. 1. Proposed location for the plant

Source: Authors' own data

https://doi.org/10.24191/mjcet.v7i2.1863

2.4 Plant layout facilities

The plant consists of a process area, atmospheric tankage, flare, utilities, parking, maintenance and warehouse areas along with offices. The size and layout of every section and the distance between sections are made using block layout methodology and was based on the Guidelines for Facility Siting and Layout (Center for Chemical Process Safety, 2003). Fig. 2 provides a detailed ethanol production plant layout. The size and distance of all these parts are critical since the footprint area from the release scenario may encompass areas outside of the process area section, such as the control room and workshop, altering the fatality percentage estimates (Ahmad et.al., 2022).

2.5 Number of people in the plant and surrounding

The number of people working in the plant, is identified using interpolation of data retrieved from a technical report published by AcuTech Process Risk Management (2016) and a work from Pérez-Fortes et al., (2016). There are two shifts in a day at the ethanol production plant. During the day shift, there are forty-eight (48) people working while during the night shift, there are twenty-six (26) people working. For the number of people outside of the production plant, the data was retrieved from Department of Statistics Malaysia (2023) where the density of people around Kuala Selangor are one hundred seventy-one people (171) for every kilometre square.

2.6 Determination of chemical hazardous and consequence scenario

According to the Guidelines for Quantitative Risk Assessment (Purple Book), a list of potential incidents has been identified for each plant (de Haag et al., 2001). The author also noted that in the case of hazardous chemicals within a mixture, each chemical should be considered as a pure substance with its own toxic, physical, and chemical properties (de Haag et al., 2001). As a result, the beginning events for continuous and instantaneous release involving hazardous chemicals in the mixture of CO-CO_2-H_2- EtOH-CH_3COOH-H_2O can be treated as pure chemicals of CO, CO_2, H_2, EtOH, and CH_3COOH. Thus, when a release occurs, the mixture will be treated as a separate event containing pure substance in the mixture which is the release of CO, CO_2, H_2, EtOH, and CH_3COOH.

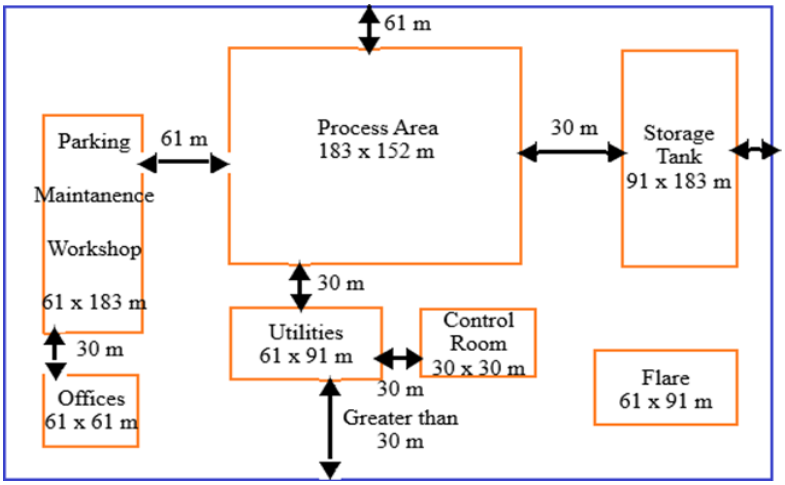

Fig. 2. Ethanol plant layout with different section size

Source: Center for Chemical Process Safety (2003)

https://doi.org/10.24191/mjcet.v7i2.1863

For the event of an instantaneous release, the event must be modelled as a totally ruptured vessel which for gas there is no air entrainment during gas expansion and for liquid there is a spreading pool which can be assumed as a large-sized hole (de Haag, 2005). For an event of a continuous release, the event must be modelled as a hole in the vessel wall (sharp orifice) which can be assumed as a small to medium-sized hole (de Haag, 2005). For instantaneous release, the size of the hole is assumed to be 160 mm. For continuous release, the size of the hole is assumed to be 10 mm and 25 mm. For carbon dioxide and carbon monoxide, both pure chemicals only have toxic characteristics with no flammable characteristics and low reactivity (Airgas, 2018; Airgas, 2020a).

Thus, the only possible scenario when a release incident happens is gas dispersion with a toxic effect. For hydrogen and ethanol, all of the pure chemicals have only flammable characteristics with classification of average to highly reactive gas (Airgas, 2020b; New Jersey Department of Health, 2007; ThermoFisher, 2022). Thus, for purely hydrogen and ethanol flammable events, the consequences event has the probability of direct ignition and delayed ignition. The event outcome case for direct ignition is jet fire, while the incident outcome cases for delayed ignition are flash fire and vapor cloud explosion (VCE) (Ahmad et al., 2022). The consequences event for solely hydrogen and ethanol hazardous events lead to direct ignition and no ignition scenarios, where jet fire and toxic fire impact are the end conclusion cases, respectively.

There will be two incidents for carbon monoxide release (gas dispersion with toxic effect and flash fire), while six incidents for hydrogen and ethanol release [gas dispersion with toxic effect, vapour cloud explosion (VCE), boiling -liquid expanding-vapour explosion (BLEVE), flash fire, jet fire and pool fire], which contribute to a total of 14 total incidents for every leakage size. The incident outcome cases are divided into day and night conditions, having stability class B and a wind speed of 2 m/s for daytime, while stability class F and a wind speed of 1 m/s for night-time. All of the scenarios are stimulated for two dominant wind directions that have blown into densely populated locations in the plant area. These people are located in the utility area, control room, office and workshop/maintenance area. Therefore, considering all the consequences of events during the day and night with wind from 2 directions, there are a total of 56 incident outcome cases evaluated. Combining the case for different leakage sizes of 10 mm, 25 mm, and 160 mm, there will be 168 incident outcomes.

2.7 Theory of consequence scenario

Theory of consequence scenario consist of several model such as source model, toxic release and dispersion model, boiling-liquid expanding vapor explosion (BLEVE), vapor cloud explosion (VCE), flash fire, jet fire and pool fire model.

Source model

Gas outflow must be characterized as subsonic or sonic based on the tank pressure, Pt to atmospheric pressure ratio, Pa as well as the ratio of gas heat capacity at constant volume and constant pressure (Casal, 2018b). The constricted pressure, mass discharge rate, discharge coefficient, area of the hole, gas density and temperature, and tank temperature must then be established.

Toxic release and dispersion models

Neutrally buoyant dispersion models are used to predict concentrations downwind of a discharge in which the gas is mixed with fresh air until the combination is neutrally buoyant (Crowl & Louvar, 2011). There are two types of neutrally buoyant vapor cloud dispersion models commonly used which are the plume and the puff models. The plume model explains the steady-state concentration of a continuous source's material while the puff model depicts the temporal concentration of material resulting from the discharge of a specific amount of material in a single release (Crowl & Louvar, 2011). Table B4 and B5 in the Appendix provides more detail on Pasquill-Gilford dispersion coefficients for plume and puff dispersion, respectively.

https://doi.org/10.24191/mjcet.v7i2.1863

Boiling liquid expanding-vapor explosion

BLEVE is a phenomenon in which a tank containing a liquid kept above its boiling point at atmospheric pressure ruptures, resulting in the explosive vaporization of a major portion of the tank contents (Crowl & Louvar, 2011). The initial phase in the development of BLEVE is when a fire develops near a tank carrying a liquid. The fire then warms up the tank wall, increasing the liquid temperature and pressure in the tank while the liquid cools the tank walls below the liquid level. If the flames reach the tank's walls or roof, where there is just vapor, the tank's metal temperature rises until the tank loses structural strength, causing the tank to break and vaporize its contents explosively (Crowl & Louvar, 2011). If a fire does not create the BLEVE, a vapor cloud may build, resulting in a VCE.

Vapor cloud explosion

VCE is a phenomenon where an explosion occurs in a sequence step in which, firstly, there will be a sudden release of a large quantity of flammable vapor (typically this occurs when a vessel, containing a superheated and pressurized liquid, ruptures), followed by dispersion of the vapor throughout the plant site while mixing with air, and ignition of the resulting vapor cloud (Crowl & Louvar, 2011). Using the Trinitrotoluene (TNT)-equivalency technique, the overpressure may be estimated by calculating the distance from the site of the explosion.

Flash fire

Due to the flash fire's short duration of time, the heat radiates is usually insignificant. Version 5.4.7 of the Aerial Location Hazardous Atmosphere (ALOHA) program does not include modelling for flash fire assessment, which has a thermal radiation impact (Ahmad et al., 2022). ALOHA, on the other hand, employs a lower flammability limit (LEL) or explosive limit in which a chemical concentration of 60% is regarded as a hazardous danger zone (Jones et al., 2013).

Jet fire

Other than secondary flames, toxicity from the fire, and smoke, the primary consequence of jet fire hazard is the thermal radiation intensity effect (Ahmad et al., 2022). In this research, the assumption has been made that the release hole may be approximated as a nozzle. Furthermore, assuming a vertical flame yields a conservative estimate since the vertical flame provides the most radiant heat flux at each receptor site. A model for predicting the effective visible flame length was collected from an article by (R Hawthorne et al., 1925). The radiative proportion of the heat of combustion is used to calculate average emissive power (Roberts, 1981). Then, using the atmospheric transmissivity, view factor, and average emissive power, the thermal radiation intensity may be computed.

Pool fire

A pool fire is a diffusion flame in which a layer of volatile liquid fuel evaporates and burns. The fuel layer can be either horizontal or floating atop a higher-density liquid, often water (Inamura et al., 1992). The heat release rate, which defines the minimum safe distance required to avoid thermal radiation burns, is the most essential physical element defining a pool fire. Because the combustion process occurs in the gas phase, the rate of heat release is restricted by the rate of evaporation of the fuel. Other physical elements, such as the depth, surface area, and form of the pool, as well as the fuel boiling point, heat of vaporization, heat of combustion, thermal conductivity, and others, influence the evaporation rate (Zhang et al., 2014).

2.8 Theory of consequence scenario

This model was performed using process simulation data via Aspen Plus version V12 to determine the density, volume, and mass fraction of chemicals in the mixture. After the result was obtained, consequence model equations were used in ALOHA software Version 5.4.7 to determine the value of toxicity, thermal

https://doi.org/10.24191/mjcet.v7i2.1863

and overpressure (Jones et al., 2013). MARPLOT version 5.1.1 program then converts these values into area footprints based on the threat zone, which calculates accurate area cover. These were deemed to be the locations affected by hazards. The proportion of deaths will be calculated by dividing the area footprints by the size of these sections. Fig. 3 shows the flowchart methodology for Consequence Analysis.

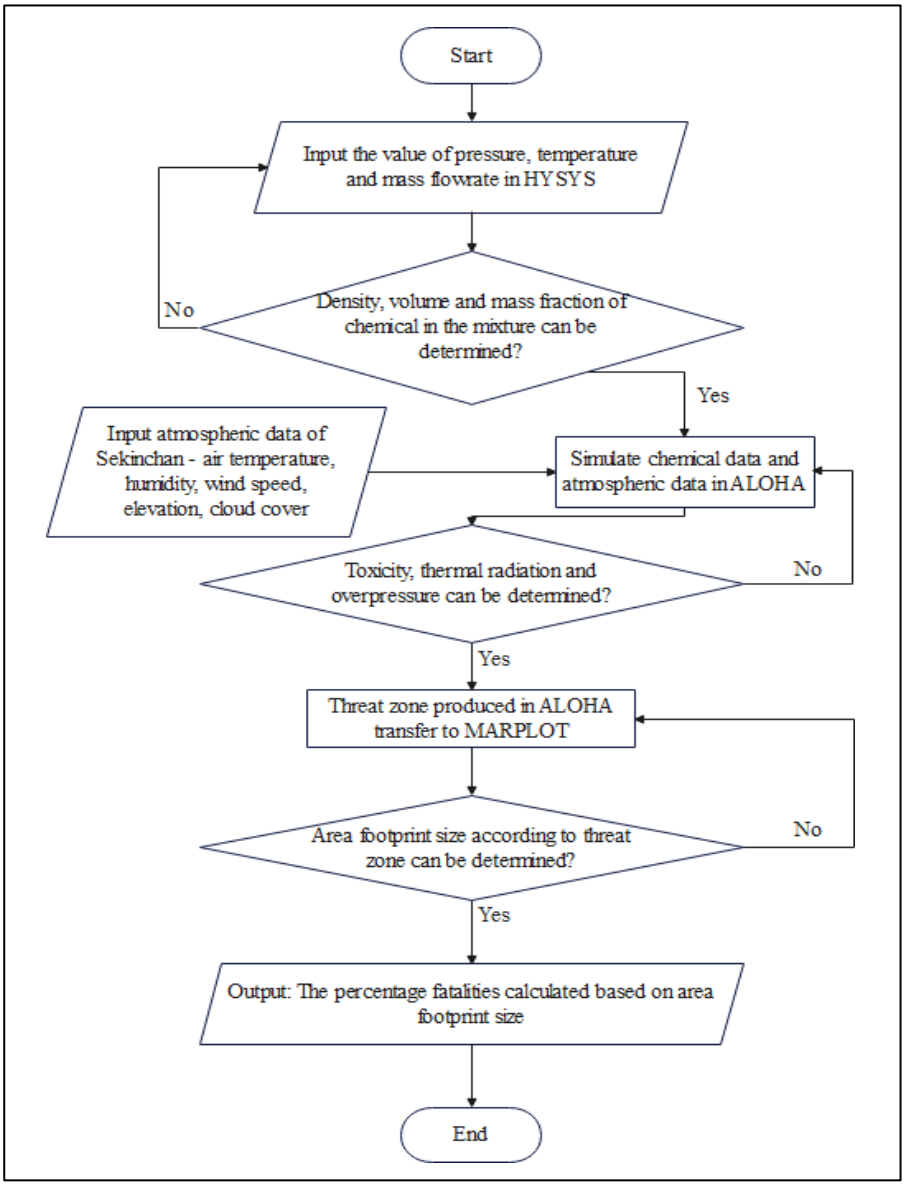

Fig. 3. Flowchart methodology for consequence analysis

Source: Ahmad et al. (2022)

https://doi.org/10.24191/mjcet.v7i2.1863

3. RESULTS AND DISCUSSION

3.1 Percentage fatalities due to release from 10 mm leakage size

There are 52 possible outcome case events at all plants for 10 mm leakage size, but only a few outcome cases resulted in fatalities. For the 10 mm leakage incident, only 16 incident outcome cases caused fatalities to people inside the plant and outside the plant. Tables 1 and 2 present the list of incident outcome case events that occurred and their subjected percentages of fatalities with their corresponding wind direction. The incident involved three different major equipment which are combustor (R-101), gasifier (R-102), and bioreactor (R-103) with the largest volume fraction of pure chemical components being H_2, CO, and C_2H_5OH, respectively. The most affected incident outcome case involved the release of ethanol as a fireball from South West (SW) to North East (NE) wind directions at night, which has a fatalities percentage of 86.77% fatalities followed by the same incident in the day from East North East (ENE) to West South West (WSW) that contributed to 81.76% fatalities. All these events occurred for Plant 1 (Reference Plant). For ethanol release with a wind direction of ENE to WSW at Plant 2, it has a percentage of fatalities inside the plant of 81.32% during daytime while at night-time the percentage of fatalities are the same. Meanwhile, for wind direction of SW to NE, the percentage of fatalities is equal to 81.32% in the daytime and for the night- time, the percentage of fatalities is equal to 86.77%. The high percentage of fireball incidents involving ethanol is due to the large amount of ethanol in the bioreactor reaching its lower flammability limit (LFL) at a temperature of 37 °C and a pressure of 1 bar. According to the National Institute for Occupational Safety and Health (NIOSH), ethanol is highly flammable and can ignite at room temperature (NIOSH, n.d.).

Hydrogen release also contributed to the fatal accident cases for both day and night in the event of flash fire and VCE. The incident of a hydrogen flash fire with a wind direction of ENE to WSW results in a fatality rate of 1.84% at a distance of 182 m for Plant 1 and 2.02% at a distance of 190 m for Plant 2, during the daytime. At night, the fatality rate is 1.76%, for both Plant 1 and Plant 2. The percentage of fatalities from a hydrogen flash fire is low because the quantity of hydrogen reaching the lower flammability limit (LFL) is insufficient to significantly ignite the flash fire, regardless of day or night conditions. While at wind direction of SW to NE, the daytime fatalities percentage is 1.84% and 2.02% for Plants 1 and 2, respectively. For night-time, the percentage of fatalities is 2.70% and 2.91% for Plant 1 and 2, respectively. For VCE events with wind direction from ENE to WSW in daytime, the percentage of fatalities is 6.70% and 7.33% for Plants 1 and 2, respectively. For night-time, the percentage of fatalities is 13.71% and 13.73% for Plants 1 and 2, respectively. While with wind direction from SW to NE at daytime, the percentage of fatalities is 6.70% and 7.33% for Plants 1 and 2, respectively. For the night-time, the percentage of fatalities is 14.42% and 14.29% for Plants 1 and 2, respectively.

Table 1. Incident outcome cases, percentage fatalities and total number of fatalities of all plants for 10 mm leakage size with wind direction from ENE to WSW

	Event	Period	Distance – Plant 1 (m)	Percentage fatalities – Plant 1	Distance – Plant 2 (m)	Percentage fatalities – Plant 2
1	H_2-Flash Fire	Day	182	1.84	190	2.02
2	H_2-Flash Fire	Night	1400	1.76	1500	1.76
3	H_2-VCE	Day	127	6.70	133	7.33
4	H_2-VCE	Night	672	13.71	691	13.73
5	CO-Toxic	Day	215	5.06	224	5.51
6	CO- Toxic	Night	2000	3.23	2100	3.14
7	Ethanol- Fireball	Day	223	81.76	223	81.32
8	Ethanol- Fireball	Night	223	81.32	223	81.32

Source: Authors' own data

https://doi.org/10.24191/mjcet.v7i2.1863

Table 2. Incident outcome cases, percentage fatalities and total number of fatalities of all plants for 10 mm leakage size with wind direction from SW to NE

	Event	Period	Distance – Plant 1 (m)	Percentage fatalities – Plant 1	Distance – Plant 2 (m)	Percentage fatalities – Plant 2
1	H_2-Flash Fire	Day	182	1.84	190	2.02
2	H_2-Flash Fire	Night	1400	2.70	1500	2.91
3	H_2-VCE	Day	127	6.70	133	7.33
4	H_2-VCE	Night	672	14.42	691	14.29
5	CO-Toxic	Day	215	5.06	224	5.51
6	CO-Toxic	Night	2000	4.51	2100	4.52
7	Ethanol- Fireball	Day	223	81.32	223	81.32
8	Ethanol- Fireball	Night	223	86.77	223	86.77

Source: Authors' own data

For carbon monoxide release, also contributed to fatal accident cases day and night in the event of toxic release. The incident for carbon monoxide toxic release at wind direction of ENE to WSW causes a percentage fatality of 5.06% and 5.51% for Plants 1 and 2, respectively, for daytime. For night-time, the percentage of fatalities is 3.23% and 3.14% for Plants 1 and 2, respectively. While at wind direction from SW to NE, the daytime fatalities percentage is 5.06% and 5.51% for Plants 1 and 2, respectively. For night-time, the percentage fatalities are 4.51% and 4.52% for Plants 1 and 2, respectively. Fig. 4 (left) and 4 (right) show the area affected footprint from ENE wind direction, for the leakage size of 10 mm and release of CO, at daytime and night-time.

The footprint during daytime affected about 9160 m^2 of the plant area and there is no footprint for the outside of the plant area, while during the night-time condition, the affected area was around 5850 m^2 of the plant area and 27,765 m^2 for the outside of the plant area. Fig. 5 (left) and 5 (right) depict the area affected footprint from the SW wind direction, for the 10 mm leakage release of CO, at daytime and night-time. The footprint during the daytime affected about 9160 m^2 of the plant area, while during the night-time condition, the affected area was around 8170 m^2 of the plant area and 173,642 m^2 for the outside of the plant area.

Fig. 4. (left) Footprint of CO released at daytime for plant 1, 10 mm leakage with 5.06% fatalities (from ENE wind direction); (right) Footprint of CO released at night-time for plant 1, 10 mm leakage with 3.23% fatalities (from ENE wind direction)

Source: Authors' own data

https://doi.org/10.24191/mjcet.v7i2.1863

Fig. 5. (left) Footprint of CO released at daytime for plant 1, 10 mm leakage with 5.06% fatalities (from SW wind direction); (right) Footprint of CO released at night-time for plant 1, 10 mm leakage with 4.51% fatalities (from SW wind direction)

Source: Authors' own data

3.2 Percentage fatalities due to release from 25 mm leakage size

As in the previous scenario, there will be 52 outcome cases events occurring at all plants for 25 mm leakage size but not all have contributed to cause fatalities. Out of these 52 events, there will be 24 incident outcome case scenarios that can cause fatalities to the people around the plant and outside the plant. Table 3 and 4 show the list of incident outcome case events that occurred. The incident involved three different major equipment which are combustor (R-101), gasifier (R-102), and bioreactor (R-103) with the largest volume fraction of pure chemical components being H_2, CO, and C_2H_5OH, respectively. Again, the most affected incident outcome case involved the release of ethanol as a fireball from SW to NE wind directions at night, which has a fatalities percentage of 86.77% fatalities followed by the same incident in the day from ENE to WSW that contributed to 81.71% fatalities, respectively. All these events occurred for Plant 2. For ethanol release with a wind direction of ENE to WSW at Plant 1, it has a percentage of fatalities inside the plant of 81.71% during daytime while at night-time the percentage of fatalities is the same. Meanwhile, for wind direction of SW to NE, the percentage of fatalities is equal to 81.71% in the daytime and for the night-time, the percentage of fatalities is also equal to 81.71%.

Hydrogen release also contributed to the fatal accident cases for both day and night in the event of toxic, flash fire, VCE, and jet fire. For wind direction from ENE to WSW, H_2-Toxic incidents demonstrate relatively low fatality rates for both day and night operations. During the day, the percentage of fatalities inside the plant is 0.58%, , and the incident occurred at a distance of 72 m from Plant 1 and 75 m from Plant 2. At night, the fatality percentage slightly increases to 2.50%. For wind direction from SW to NE, the incidents resulted in negligible fatalities (ranging from 0.28% to 0.92%). Lower fatalities for hydrogen toxic because hydrogen is generally considered non-toxic, although it can act as an asphyxiant in high concentrations (NIOSH, n.d.). According to the Occupational Safety and Health Administration (OSHA, n.d.), its primary hazards stem from its flammability and potential for explosive reactions.

The incidents occurred at distances of 72 to 75 m from Plant 1 and 453 to 461 m from Plant 2. These incidents indicate that H2-Toxic accidents have relatively minor consequences, but safety measures should still be in place to mitigate potential harm to personnel and the environment. For flash fire incidents with wind direction from ENE to WSW, H_2-Flash Fire incidents show moderate fatality rates. During the day, the percentage of fatalities inside the plant is 4.73%, at a distance of 409 m from Plant 1 and 422 m from

https://doi.org/10.24191/mjcet.v7i2.1863

Plant 2. At night, the percentage of fatalities remains similar at 1.89%, resulting in at a distance of 1900 m from both plants. For wind direction from SW to NE, during the day, the percentage of fatalities ranges from 2.95% to 6.15%. Accidents at night show similar trends, with fatalities ranging from 0.69 to 0.71%. The accidents occurred at distances of 409 to 422 m from Plant 1 and 1900 m from both plants. While these accidents are not as severe as Ethanol-Fireball incidents, they still underscore the importance of robust safety measures and emergency response plans during H_2-Flash Fire events. For VCE incidents, H_2-VCE incidents demonstrate higher fatality rates compared to H_2-Flash Fire incidents. During the day, the percentage of fatalities is 26.58%. The incident occurs at a distance of 277 m from Plant 1 and 286 m from Plant 2. At night, the percentage of fatalities is 12.55%, at a distance of 1600 m from both plants. For wind direction from SW to NE, during the day, the percentage of fatalities ranges from 13.61% to 28.35%. At night, the percentage of fatalities inside the plant remains high at 15.32% to 15.40%. H_2-VCE accidents occurred at distances of 277 to 286 m from Plant 1 and 1600 m from both plants. These findings indicate that H_2-VCE accidents have substantial consequences, particularly during night-time operations, highlighting the need for enhanced safety measures and emergency preparedness. For jet fire incidents with wind direction from ENE to WSW, H_2- Jet Fire incidents show moderate fatality rates. During the day, the percentage of fatalities is 3.46%, at a distance of 45 m from both plants. At night, the percentage of fatalities remains consistent at 3.46%, a distance of 47 m from both plants. For wind direction from SW to NE, the percentage of fatalities ranges from 0.90% to 1.66%. The accidents occurred at distances of 45 m from both plants. While H_2-Jet Fire incidents appear less severe compared to Ethanol-Fireball, H_2-VCE, and H_2-Flash Fire events, it is crucial to implement safety protocols to prevent potential harm to personnel.

Carbon monoxide release also contributed to fatal accident cases day and night in an event of toxic release. The incident for carbon monoxide toxic release at wind direction of ENE to WSW, during the day, the percentage of fatalities 10.25%, and the incident occurs at a distance of 526 m from Plant 1 and 545 m from Plant 2. At night, the percentage of fatalities is 3.59%, at a distance of 3400 m from both plants. For wind direction from SW to NE, during the day, the percentage of fatalities inside the plant ranges from 6.29% to 13.11%. At night, the percentage of fatalities ranges from 1.27% to 5.17%. These incidents occurred at distances of 526 to 545 m from Plant 1 and 3400 m from both plants. These accidents indicate that CO-toxic incidents can have significant consequences both inside and outside the plant, necessitating robust safety measures and emergency response plans.

Table 3. Incident outcome cases, percentage fatalities and total number of fatalities of all plants for 25 mm leakage size with wind direction from ENE to WSW

	Event	Period	Distance – Plant 1 (m)	Percentage fatalities – Plant 1	Distance – Plant 2 (m)	Percentage fatalities – Plant 2
1	H_2-Toxic	Day	72	0.58	75	0.61
2	H_2-Toxic	Night	453	2.50	461	2.65
3	H2-Flash Fire	Day	409	4.73	422	4.88
4	H_2-Flash Fire	Night	1900	1.89	1900	1.86
5	H_2-VCE	Day	277	26.58	286	27.49
6	H_2-VCE	Night	1600	12.55	1600	12.34
7	I_2-Jet Fire	Day	45	3.46	47	3.74
8	I_2-Jet Fire	Night	45	3.46	47	3.74
9	CO-Toxic	Day	526	10.25	545	10.52
10	CO-Toxic	Night	3400	3.59	3400	3.54
11	Ethanol-Fireball	Day	223	81.71	223	81.71
12	Ethanol-Fireball	Night	223	81.71	223	81.32

Source: Authors' own data

https://doi.org/10.24191/mjcet.v7i2.1863

Table 4. Incident outcome cases, percentage fatalities and total number of fatalities of all plants for 25 mm leakage size with wind direction from SW to NE

	Event	Period	Distance – Plant 1 (m)	Percentage fatalities – Plant 1	Distance – Plant 2 (m)	Percentage fatalities – Plant 2
1	H_2-Toxic	Day	72	0.58	75	0.61
2	H_2-Toxic	Night	453	3.53	461	3.57
3	H_2-Flash Fire	Day	409	6.15	422	6.31
4	H_2-Flash Fire	Night	1900	2.72	1900	2.67
5	H_2-VCE	Day	277	28.35	286	29.66
6	H_2-VCE	Night	1600	15.32	1600	15.40
7	I_2-Jet Fire	Day	45	3.46	47	3.74
8	I_2-Jet Fire	Night	45	3.46	47	3.74
9	CO-Toxic	Day	526	13.11	545	13.49
10	CO-Toxic	Night	3400	5.17	3400	4.90
11	Ethanol- Fireball	Day	223	81.71	223	81.32
12	Ethanol- Fireball	Night	223	81.71	223	86.77

Source: Authors' own data

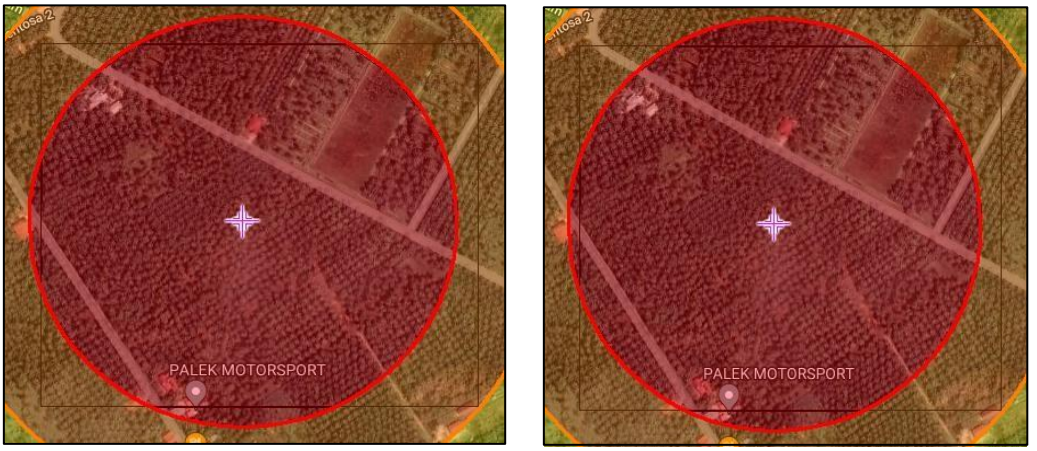

Fig. 6. (left) Footprint of Ethanol released at daytime for plant 1, 25 mm leakage with 81.71% fatalities (from ENE wind direction); (right) Footprint of Ethanol released at daytime for plant 1, 25 mm leakage with 81.71% fatalities (from SW wind direction)

Source: Authors' own data

Fig. 6 (left) and (right) shows the area affected footprint from ENE and SW wind direction, for the leakage size of 25 mm and release of ethanol at daytime and night-time. The footprint during daytime affected about 147,872 m^2 of the plant area and 9204 m^2 for the outside of the plant area, while during the night-time condition, the affected area was the same as the daytime condition.

3.3 Percentage fatalities due to release from 160 mm leakage size

Same as the previous scenario, there will be 52 outcome cases events occurring at all plants for 160 mm leakage size but not all have contributed to cause fatalities. Out of these 52 events, there will be 36 incident outcome case scenarios that can cause fatalities to the people around the plant and outside the plant.

https://doi.org/10.24191/mjcet.v7i2.1863

Tables 5 and 6 show the list of incident outcome case events that occurred. The incident involved three different major equipment which are combustor (R-101), gasifier (R-102), and bioreactor (R-103) with the largest volume fraction of pure chemical components being H_2, CO, and C_2H_5OH, respectively. The most affected incident outcome case involved the release of CO as toxic from SW to NE wind directions at night, which has a fatalities percentage of 5.25% fatalities followed by the same incident in the day from ENE to WSW that contributed to 13.77% fatalities. All these events occurred for Plant 1. For CO release with a wind direction of ENE to WSW at Plant 2, it has a percentage of 13.61% while at night-time the percentage of fatalities is 3.79%. Meanwhile, for wind direction of SW to NE, the percentage of fatalities is equal to 16.62% in the daytime for the night- time, the percentage of fatalities is also equal to 5.35%.

Hydrogen release also contributed to the fatal accident cases for both day and night in the event of toxic, flash fire, VCE, and jet fire. For wind direction from ENE to WSW, H_2-Toxic incidents exhibit relatively low fatality rates during both day and night operations. The percentage of fatalities inside the plant remains consistent, ranging from 1.46% to 2.96%. Accidents occur at a distance of 115 m from both plants during both periods. The incidents resulted in limited fatalities inside the plant, ranging from 0.70 to 0.77. For wind direction from SW to NE, H_2-Toxic accidents exhibit relatively low fatality rates during both day and night operations. The percentage of fatalities ranges from 1.46% to 3.97%. These results indicate that H_2-Toxic incidents have limited impacts on personnel and neighbouring areas. For flash fire incidents with wind direction from ENE to WSW, H_2- Flash Fire incidents show moderate fatality rates, with the percentage of fatalities inside the plant ranging from 5.50% to 5.56%. Accidents occur at a distance of 592 m from both plants during the day and night. For wind direction from SW to NE, the percentage of fatalities ranges from 7.68% to 14.36%.

Table 5. Incident outcome cases, percentage fatalities and total number of fatalities of all plants for 160 mm leakage size with wind direction from ENE to WSW

	Event	Period	Distance – Plant 1 (m)	Percentage fatalities – Plant 1	Distance – Plant 2 (m)	Percentage fatalities – Plant 2
1	H_2-Toxic	Day	115	1.46	115	1.46
2	H_2-Toxic	Night	538	2.77	538	2.96
3	H_2-Flash Fire	Day	592	5.50	592	5.56
4	H_2-Flash Fire	Night	2000	1.92	2000	1.89
5	H_2-VCE	Day	528	33.67	528	33.59
6	H_2-VCE	Night	1700	11.62	1700	13.73
7	H_2-Jet Fire	Day	100	17.16	105	18.83
8	H_2-Jet Fire	Night	100	17.14	104	18.82
9	CO-Toxic	Day	1000	13.77	1000	13.61
10	CO-Toxic	Night	3800	3.66	3800	3.79
11	CO-Flash Fire	Day	133	0.99	133	0.99
12	CO-Flash Fire	Night	599	1.38	599	1.68
13	CO-Jetfire	Day	30	1.19	31	1.35
14	CO-Jetfire	Night	26	1.01	28	1.20
15	Ethanol-Pool Fire	Day	29	1.34	29	1.34
16	Ethanol- Pool Fire	Night	28	1.34	28	1.34
17	Ethanol- Fireball	Day	223	81.71	223	81.71
18	Ethanol- Fireball	Night	223	81.71	223	81.71

Source: Authors' own data

https://doi.org/10.24191/mjcet.v7i2.1863

Table 6. Incident outcome cases, percentage fatalities and total number of fatalities of all plants for 160 mm leakage size with wind direction from SW to NE

	Event	Period	Distance – Plant 1 (m)	Percentage fatalities – Plant 1	Distance – Plant 2 (m)	Percentage fatalities – Plant 2
1	H_2-Toxic	Day	115	1.46	115	1.46
2	H_2-Toxic	Night	538	3.97	538	3.90
3	H_2-Flash Fire	Day	592	7.68	592	7.80
4	H_2-Flash Fire	Night	2000	2.86	2000	2.83
5	H_2-VCE	Day	528	36.18	528	35.82
6	H_2-VCE	Night	1700	14.36	1700	14.68
7	H_2-Jet Fire	Day	100	17.16	105	18.82
8	H_2-Jet Fire	Night	100	17.13	104	18.82
9	CO-Toxic	Day	1000	16.99	1000	16.62
10	CO-Toxic	Night	3800	5.25	3800	5.35
11	CO-Flash Fire	Day	133	0.99	133	0.99
12	CO-Flash Fire	Night	599	2.12	599	2.26
13	CO-Jetfire	Day	30	1.19	31	1.35
14	CO-Jetfire	Night	26	1.01	28	1.20
15	Ethanol- Pool Fire	Day	29	1.34	29	1.34
16	Ethanol- Pool Fire	Night	28	1.34	28	1.34
17	Ethanol- Fireball	Day	223	81.71	223	81.71
18	Ethanol- Fireball	Night	223	81.71	223	81.71

Source: Authors' own data

For VCE incidents, H_2- VCE incidents demonstrate substantial fatality rates, particularly during night-time operations. The percentage of fatalities ranges from 11.62% to 33.67%. Accidents occur at a distance of 528 m from both plants during the day and 1700 m during the night. For wind direction from SW to NE, the percentage of fatalities inside the plant ranges from 35.82% to 36.18%. These findings highlight the critical need for stringent safety measures, proactive risk assessment, and emergency response planning to prevent or mitigate the impact of H_2-VCE incidents, especially during night-time operations. For jet fire incidents with wind direction from ENE to WSW, H_2-Jet Fire incidents demonstrate moderate fatality rates during both day and night. The percentage of fatalities ranges from 17.14% to 18.83%. Accidents occur at a distance of 100 to 105 m from Plant 1 and 100 to 104 m from Plant 2. For wind direction from SW to NE, the percentage of fatalities ranges from 17.13% to 18.82%.

For ethanol release, it also contributed to fatal accident cases day and night in the event of pool fire and fireball release. The incident for ethanol pool fire and fireball release at wind direction of ENE to WSW, Ethanol-Pool Fire and Ethanol-Fireball incidents demonstrate relatively low fatality rates during both day and night operations. The percentage of fatalities ranging from 1.34% to 81.71% for Ethanol-Pool Fire and from 21.24% to 81.71% for Ethanol-Fireball. Accidents occur at a distance of 28 to 29 m for both events. For wind direction from SW to NE, Ethanol-Pool Fire and Ethanol-Fireball incidents demonstrate relatively low fatality rates during both day and night operations. The percentage of fatalities ranging from 1.34% to 81.71% for Ethanol Pool Fire and from 21.24% to 81.71% for Ethanol Fireball. Accidents occur at a distance of 28 to 29 m for both events.

Fig. 7 (left) and (right) show the area affected footprint from ENE wind direction, for the leakage size of 160 mm and release of H_2 as VCE at daytime and night- time. The footprint during daytime was affected about 60,939 m^2 of the plant area and 67,707 m^2 for the outside of the plant area, while during the night-

https://doi.org/10.24191/mjcet.v7i2.1863

time condition, the affected area was about 21,027 m^2 of the plant area and 102,103 m^2 for the outside of the plant area.

Fig. 8 (left) and (right) depict the area affected footprint from the SW wind direction, for the 160 mm leakage release of H_2 as VCE at daytime and night-time. The footprint during daytime was affected about 65,474 m^2 of the plant area and 63,175 m^2 for the outside of the plant area, while during the night-time condition, the affected area was about 25,995 m^2 of the plant area and 333,064 m^2 for the outside of the plant area.

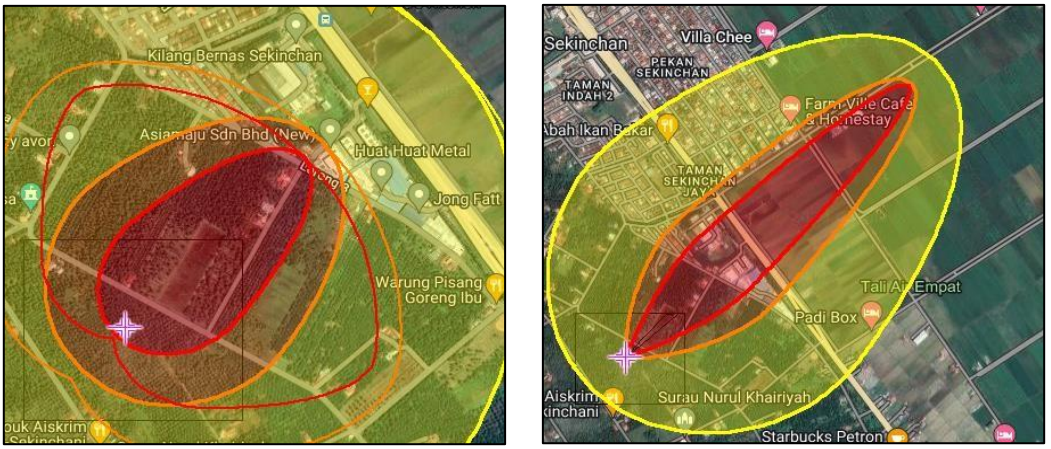

Fig. 7. (left) 9 Footprint of H2 released as VCE at daytime for plant 1, 160 mm leakage with 36.18% fatalities (from SW wind direction; (right) Footprint of H2 released as VCE at night-time for plant 1, 160 mm leakage with 14.36% fatalities (from SW wind direction)

Source: Authors' own data

Fig. 8. (left) Footprint of H_2 released as VCE at daytime for plant 1, 160 mm leakage with 33.67% fatalities (from ENE wind direction; (right) Footprint of H2 released as VCE at night-time for plant 1, 160 mm leakage with 11.62% fatalities (from ENE wind direction)

Source: Authors' own data

https://doi.org/10.24191/mjcet.v7i2.1863

4. ANALYSIS OF THE RESULTS

4.1 Comparison of chemical release

Chemicals that could be released and have consequential effects on the workers inside and outside the plant are CO, H_2, and Ethanol. Among these, Ethanol has been identified as the one with the most extensive affected area, marked with a red zone, compared to H_2 and CO. This has been proven by the highest percentage of fatalities, 86.77%, for Plant 2 during night-time conditions when 25 mm leak sizes occurred, leading to a fireball event. The primary factor for this is the high flammability of Ethanol, which can ignite and produce a fire even at room temperature. Additionally, Ethanol's vapor is heavier than air, allowing it to spread quickly and increase the risk of ignition over a larger area. This characteristic makes it particularly hazardous in enclosed spaces or areas with poor ventilation, further emphasizing the need for stringent safety measures to prevent and control potential leaks.

4.2 Comparison of different operating temperature condition

Plant 1 and 2 reactors operate at different temperature conditions: for Plant 1, the R-101 (H_2 release) operates at 700 °C. the R-102 (CO release) operates at 700 °C and the R-103 (Ethanol release) operates at 37 °C. For Plant 2, the R-101 (H_2 release) operates at 700 °C, the R-102 (CO release) operates at 900 °C and the R-103 (Ethanol release) operates at 30 °C. Thus, the percentage of fatalities for each plant caused by the toxicity event is not significantly different. For example, in the release incident involving a 160 mm leak size with wind blowing from the southwest, the number of fatalities is 16.99% for Plant 1 and 16.22% for Plant 2. Therefore, higher temperature conditions do not have a substantial effect on fatalities during CO release incidents.

5. CONCLUSIONS

In this research, the highest fatality percentage and number of fatalities in the two plants were associated with fireball incident events due to the release of ethanol from a 25 mm leak hole at night in Plant 2, where the wind direction blew from SW to NE. This event resulted in an 86.77% fatality rate. Meanwhile, an increase in temperature did not show much difference in the percentage of fatalities across all incidents. The findings of this study indicate that bioreactors, where ethanol is the main chemical, have the highest fatality rates and therefore require more stringent risk reduction measures. Additionally, the analysis enables safety engineers to prioritize emergency response plans concerning temperature variations. Ultimately, this study serves as a benchmark for recommending suitable locations for ethanol plants, thereby minimizing the risk of fatalities or injuries to nearby residents and protecting the environment from potential incidents. Furthermore, implementing advanced monitoring systems and regular safety drills can significantly enhance preparedness and reduce the impact of such hazardous events.

ACKNOWLEDGEMENTS/FUNDING

The authors gratefully acknowledge the Universiti Teknologi MARA for providing funding under the Geran Penyelidikan Myra (600-RMC 5/3/GPM (030/2023)). Additionally, the authors would like to express their gratitude to the School of Chemical Engineering, College of Engineering, University Teknologi MARA (UiTM) for their support in this research.

https://doi.org/10.24191/mjcet.v7i2.1863

CONFLICT OF INTEREST STATEMENT

The authors agree that this research was conducted in the absence of any self-benefits, commercial or financial conflicts and declare the absence of conflicting interests with the funders research.

AUTHORS' CONTRIBUTIONS

Muhammad Saber Khairunnizam: Data curation; Formal analysis; Investigation; Methodology; Resources; Software; Visualization; and Roles/Writing - original draft; **Mohd Aizad Ahmad**: Conceptualization; Funding acquisition; Methodology; Project administration; Resources; Software; Supervision; Validation; Visualization; Roles/Writing - original draft; and Writing - review & editing; **Zulkifli Abdul Rashid**: Funding acquisition; Methodology; Resources; Software; Supervision; Validation; **Nur Adlina Azhari**: Project administration; Resources; Software; and Writing - review & editing.

REFERENCES

Acharya, B., Roy, P., & Dutta, A. (2014). Review of syngas fermentation processes for bioethanol. *Biofuels*, *5*(5), 551–564. https://doi.org/10.1080/17597269.2014.1002996

AcuTech Consulting Group. (2017). Quantitative risk assessment final report prepared for NW Innovation Works, Port of Kalama, WA. https://pdf4pro.com/view/quantitative-risk-assessment-final-report-dc195.html

Ahmad, M. A., Rashid, Z. A., El-Harbawi, M., & Al-Awadi, A. S. (2022). High-pressure methanol synthesis case study: safety and environmental impact assessment using consequence analysis. *International Journal of Environmental Science and Technology*, *19*(9), 8555–8572. https://doi.org/10.1007/s13762-021-03724-1

Ahmed, I. I., & Gupta, A. K. (2010). Pyrolysis and gasification of food waste: Syngas characteristics and char gasification kinetics. *Applied Energy*, *87*(1), 101–108. https://doi.org/10.1016/j.apenergy.2009.08.032

Airgas (2018). *Carbon Dioxide SDS*. https://www.airgas.com/msds/001013.pdf

Airgas (2020a). *Carbon Monoxide SDS*. https://www.airgas.com/msds/001014.pdf

Airgas (2020b). *Hydrogen SDS*. https://www.airgas.com/msds/001026.pdf

Casal, J. (2018a). Chapter 11 - Quantitative Risk Analysis. *Evaluation of the Effects and Consequences of Major Accidents in Industrial Plants* (pp. 439– 481). Elsevier. https://doi.org/10.1016/b978-0-444-63883-0.00011-3

Casal, J. (2018b). Chapter 2 - Source Term. *Evaluation of the Effects and Consequences of Major Accidents in Industrial Plants* (pp. 25–74). Elsevier. https://doi.org/10.1016/B978-0-444-63883-0.00002-2

Center for Chemical Process Safety. (2003). Guidelines for Facility Siting and Layout. Wiley-AIChE.

Crowl, D. A., & Louvar, J. F. (2011). *Chemical process safety: Fundamentals with applications*. Prentice Hall.

de Haag, P. U., Ale, B. J. M., & Post, J. G. (2001). T10-1 - The 'Purple Book': Guideline for quantitative risk assessment in the Netherlands. *Loss Prevention and Safety Promotion in the Process Industries* (pp. 1429-1438). Elsevier. https://doi.org/10.1016/B978-044450699-3/50053-7

https://doi.org/10.24191/mjcet.v7i2.1863

Department of Statistics Malaysia. (2023). P.096 Kuala Selangor: Population and housing census 2020. https://open.dosm.gov.my/dashboard/kawasanku/Selangor/parlimen/P.096%20Kuala%20Selangor

Fang, K., Li, D., Lin, M., Xiang, M., Wei, W., & Sun, Y. (2009). A short review of heterogeneous catalytic process for mixed alcohols synthesis via syngas. *Catalysis Today*, *147*(2), 133–138. https://doi.org/10.1016/j.cattod.2009.01.038

Griffin, D. W., & Schultz, M. A. (2012). Fuel and chemical products from biomass syngas: A comparison of gas fermentation to thermochemical conversion routes. *Environmental Progress and Sustainable Energy*, *31*(2), 219–224. https://doi.org/10.1002/ep.11613

Hawthorne, W. R., Weddell, D. S., & Hottel, H. C. (1948, January). Mixing and combustion in turbulent gas jets. In *Symposium on Combustion and Flame, and Explosion Phenomena* (Vol. 3, No. 1, pp. 266-288). Elsevier. https://doi.org/10.1016/S1062-2896(49)80035-3

Heikkilä, A.-M. (1999). *Inherent safety in process plant design: An index-based approach* [Doctoral Dissertation, VTT Technical Research Centre of Finland, Aalto University]. Aalto University. https://aaltodoc.aalto.fi/handle/123456789/2516

Inamura, T., Saito, K., & Tagavi, K. A. (1992). A study of boilover in liquid pool fires supported on water. part II: Effects of in-depth radiation absorption. *Combustion Science and Technology*, *86*(1–6), 105–119. https://doi.org/10.1080/00102209208947190

Jones, R., Lehr, W., Simecek-Beatty, D., & Reynolds, M. (2013). ALOHA® (Areal Locations of Hazardous Atmospheres) 5.4.4: Technical Documentation. https://response.restoration.noaa.gov/sites/default/files/ALOHA_Tech_Doc.pdf

Liguori, R., Ventorino, V., Pepe, O., & Faraco, V. (2016). Bioreactors for lignocellulose conversion into fermentable sugars for production of high added value products. *Applied Microbiology and Biotechnology 100*(2), 597–611. https://doi.org/10.1007/s00253-015-7125-9

Michailos, S., Parker, D., & Webb, C. (2017). *Design, Sustainability Analysis and Multiobjective Optimisation of Ethanol Production via Syngas Fermentation*. MPRA Paper 87640, University Library of Munich, Germany.

National Institute for Occupational Safety and Health (NIOSH). Ethyl Alcohol. NIOSH Pocket Guide to Chemical Hazards. https://www.cdc.gov/niosh/npg/npgd0262.html

New Jersey Department of Health. (2007). *Right to Know Hazardous Substance Fact Sheet (Acetic Acid)*. https://www.nj.gov/health/eoh/rtkweb/documents/fs/0004.pdf

Occupational Safety and Health Administration. (n.d.). *Hydrogen*. 29 e-CFR § 1910.103. https://www.osha.gov/laws-regs/regulations/standardnumber/1910/1910.103

Pardo-Planas, O., Atiyeh, H. K., Phillips, J. R., Aichele, C. P., & Mohammad, S. (2017). Process simulation of ethanol production from biomass gasification and syngas fermentation. *Bioresource Technology*, *245*, 925–932. https://doi.org/10.1016/j.biortech.2017.08.193

Pérez-Fortes, M., Schöneberger, J. C., Boulamanti, A., & Tzimas, E. (2016). Methanol synthesis using captured CO2 as raw material: Techno-economic and environmental assessment. *Applied Energy*, *161*, 718–732. https://doi.org/10.1016/j.apenergy.2015.07.067

Roberts, A. F. (1981). Thermal radiation hazards from releases of LPG from pressurised storage. *Fire Safety Journal 4*(3), 197-212. https://doi.org/10.1016/0379-7112(81)90018-7

https://doi.org/10.24191/mjcet.v7i2.1863

Srinivasan, R., & Nhan, N. T. (2008). A statistical approach for evaluating inherent benign-ness of chemical process routes in early design stages. *Process Safety and Environmental Protection*, *86*(3), 163–174. https://doi.org/10.1016/j.psep.2007.10.011

ThermoFisher (2022). *Ethanol SDS*.

Vuthaluru, H. B. (2004). Thermal behaviour of coal/biomass blends during co-pyrolysis. *Fuel Processing Technology*, *85*(2–3), 141–155. https://doi.org/10.1016/S0378-3820(03)00112-7

Yang, Y., Wang, G., Peng, C., Deng, Q., Yu, Y., He, X., Hu, T., Jiang, L., Shan, S., Zheng, Y., Zhi, Y., & Su, H. (2023). Microwave-assisted synthesis of l-aspartic acid-based metal organic aerogel (MOA) for efficient removal of oxytetracycline from aqueous solution. *Applied Surface Science*, *610*, Article 155608. https://doi.org/10.1016/j.apsusc.2022.155608

Zhang, M., Song, W., Wang, J., & Chen, Z. (2014). Accident consequence simulation analysis of pool fire in fire dike. *Procedia Engineering*, *84*, 565–577. https://doi.org/10.1016/j.proeng.2014.10.469

Zhang, Y., Wan, L., Guan, J., Xiong, Q., Zhang, S., & Jin, X. (2020). A Review on Biomass Gasification: Effect of Main Parameters on Char Generation and Reaction. *Energy and Fuels*, *34*(11), 13438–13455. https://doi.org/10.1021/acs.energyfuels.0c02900

https://doi.org/10.24191/mjcet.v7i2.1863

Appendix

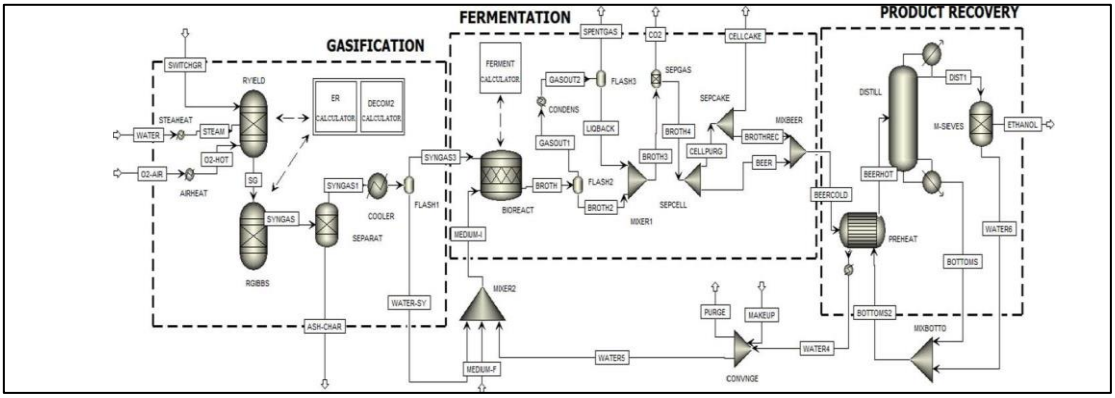

Figure A1: Process flow diagram for ethanol production of reference plant (plant 1)

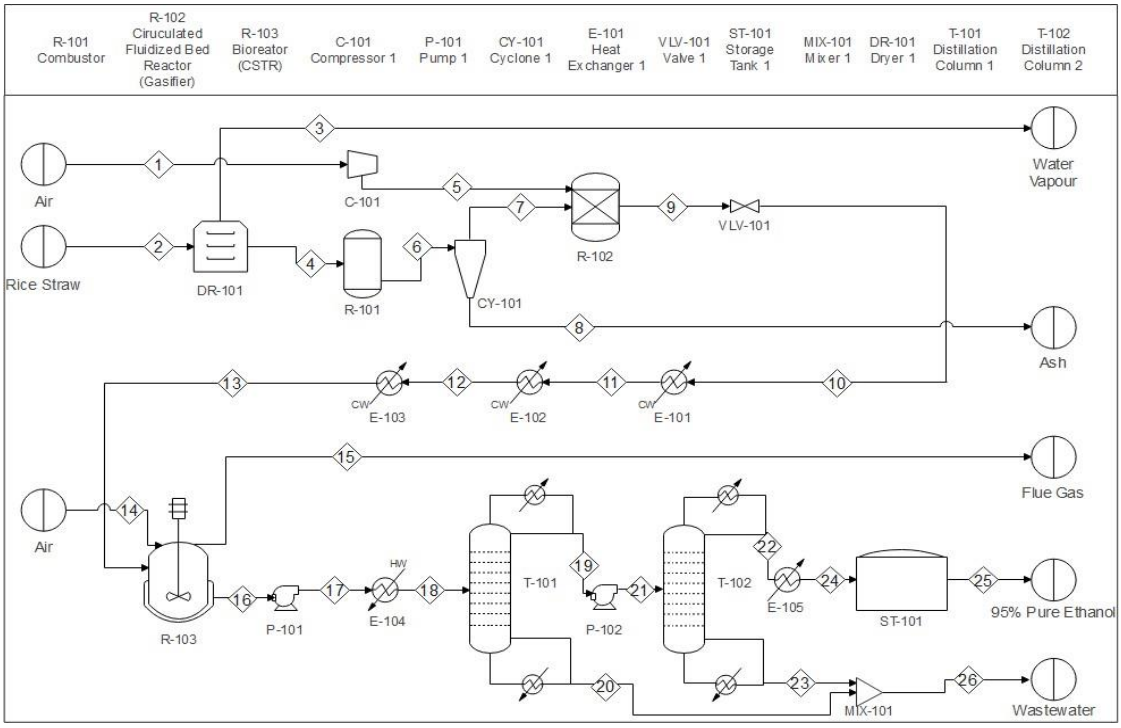

Figure A2: Process flow diagram for ethanol production of plant 2

https://doi.org/10.24191/mjcet.v7i2.1863

Table B1: Process condition of the reference plant

		Material			
Stream Name	**Units**	**Switchgrass**	**Steam**	**O_2 Hot**	**SG**
Total Stream					
Temperature	C	100.00	507.46	700.00	700.00
Pressure	bar	1.00	20.00	1.00	20.00
Mass Vapor Fraction		0.00	1.00	0.49	0.49
Mass Liquid Fraction		0.00	0.00	0.00	0.00
Mass Solid Fraction		1.00	0.00	0.51	0.51
Mass Flows	kg/hr	50000.00	25000.00	50000.00	49500.00
		Mass Fractions			
H_2		0.0000	0.0000	0.0000	0.0646
CH_4		0.0000	0.0000	0.0000	0.0000
CO		0.0000	0.0000	0.0000	0.0000
CO_2		0.0000	0.0000	0.0000	0.0000
O_2		0.0000	0.0000	1.0000	0.4269
N_2		0.0000	0.0000	0.0000	0.0014
H_2S		0.0000	0.0000	0.0000	0.0000
H_2O		0.0000	1.0000	0.0000	0.0000
Cl_2		0.0000	0.0000	0.0000	0.0000
SWITCHGRASS		1.0000	0.0000	0.0000	0.0000
ASH		0.0000	0.0000	0.0000	0.0000
C		0.0000	0.0000	0.0000	0.5063
S		0.0000	0.0000	0.0000	0.0008
CH_3COOH		0.0000	0.0000	0.0000	0.0000
C_2H_5OH		0.0000	0.0000	0.0000	0.0000

https://doi.org/10.24191/mjcet.v7i2.1863

Table B1: Continued

Material				
Stream Name	**Units**	**Syngas**	**Medium-1**	**Broth**
Total Stream				
Temperature	C	37	37	37
Pressure	bar	1	1	1
Mass Vapor Fraction		0.00	0.00	0.00
Mass Liquid Fraction		1.00	1.00	1.00
Mass Solid Fraction		0.00	0.00	0.00
Mass Flows	kg/hr	16948.31	17511.46	34459.77
Mass Fractions				
H_2		0.3552	-	-
CH_4		0.0000	-	-
CO		0.3268	-	-
CO_2		0.2667	-	-
O_2		0.0000	-	-
N_2		0.0000	-	-
H_2S		0.0000	-	-
H_2O		0.4182	-	0.6000
Cl_2		0.0000	-	-
RICESTRAW		0.0000	-	-
ASH		0.0000	-	-
C		0.0000	-	-
S		0.0000	-	-
CH_3COOH		0.0000	-	0.0387
C_2H_5OH		0.0000	-	0.3613

https://doi.org/10.24191/mjcet.v7i2.1863

Table B2: Process condition of the plant 2.

		Material			
Stream Name	**Units**	**4**	**5**	**6**	**7**
Total Stream					
Temperature	C	100.00	507.46	700.00	900.00
Pressure	bar	1.00	20.00	1.00	1.00
Mass Vapor Fraction		0.00	1.00	0.49	0.49
Mass Liquid Fraction		0.00	0.00	0.00	0.00
Mass Solid Fraction		1.00	0.00	0.51	0.51
Mass Enthalpy	kJ/kg	-5421.41	506.76	1218.81	1232.65
Mass Density	gm/cc	1.25	0.01	0.00	0.00
Enthalpy Flow	kW	-75297.40	18440.41	16927.92	16948.96
Mass Flows	kg/hr	50000.00	131000.00	50000.00	49500.00
H_2	kg/hr	0.00	0.00	3200.00	3200.00
CH_4	kg/hr	0.00	0.00	0.00	0.00
CO	kg/hr	0.00	0.00	0.00	0.00
CO_2	kg/hr	0.00	0.00	0.00	0.00
O_2	kg/hr	0.00	27510.00	21130.00	21130.00
N_2	kg/hr	0.00	103490.00	70.00	70.00
H_2S	kg/hr	0.00	0.00	0.00	0.00
H_2O	kg/hr	0.00	0.00	0.00	0.00
Cl_2	kg/hr	0.00	0.00	0.00	0.00
RICESTRAW	kg/hr	50000.00	0.00	0.00	0.00
ASH	kg/hr	0.00	0.00	500.00	0.00
C	kg/hr	0.00	0.00	25060.00	25060.00
S	kg/hr	0.00	0.00	40.00	40.00
CH_3COOH	kg/hr	0.00	0.00	0.00	0.00
C_2H_5OH	kg/hr	0.00	0.00	0.00	0.00
		Mass Fractions			
H_2		0.0000	0.0000	0.0640	0.0646
CH_4		0.0000	0.0000	0.0000	0.0000
CO		0.0000	0.0000	0.0000	0.0000
CO_2		0.0000	0.0000	0.0000	0.0000
O_2		0.0000	0.2100	0.4226	0.4269
N_2		0.0000	0.7900	0.0014	0.0014
H_2S		0.0000	0.0000	0.0000	0.0000
H_2O		0.0000	0.0000	0.0000	0.0000
Cl_2		0.0000	0.0000	0.0000	0.0000
RICESTRAW		1.0000	0.0000	0.0000	0.0000
ASH		0.0000	0.0000	0.0100	0.0000
C		0.0000	0.0000	0.5012	0.5063
S		0.0000	0.0000	0.0008	0.0008
CH_3COOH		0.0000	0.0000	0.0000	0.0000
C_2H_5OH		0.0000	0.0000	0.0000	0.0000
Volume Flow	l/min	666.26	246306.51	3034660.25	3034657.86

https://doi.org/10.24191/mjcet.v7i2.1863

Table B2: continued

		Material			
Stream Name	**Units**	**9**	**13**	**14**	**15**
Total Stream					
Temperature	C	900.00	30.00	30.00	30.00
Pressure	bar	20.00	1.00	1.00	1.00
Mass Vapor Fraction		1.00	1.00	1.00	1.00
Mass Liquid Fraction		0.00	0.00	0.00	0.00
Mass Solid Fraction		0.00	0.00	0.00	0.00
Mass Enthalpy	kJ/kg	-1533.90	-2683.95	NA	NA
Mass Density	gm/cc	0.0050	0.0010	NA	NA
Enthalpy Flow	kW	-76908.37	-134570.95	53.56	4081.45
Mass Flows	kg/hr	180500.63	180500.63	7618.36	171195.05
H_2	kg/hr	2186.57	2186.57	0.00	1071.06
CH_4	kg/hr	352.15	352.15	0.00	351.97
CO	kg/hr	43318.25	43318.25	0.00	24220.22
CO_2	kg/hr	22797.79	22797.79	0.00	34312.30
O_2	kg/hr	0.00	0.00	1774.32	1780.14
N_2	kg/hr	103560.00	103560.00	5844.04	109416.03
H_2S	kg/hr	42.51	42.51	0.00	43.32
H_2O	kg/hr	8243.36	8243.36	0.00	0.00
Cl_2	kg/hr	0.00	0.00	0.00	0.00
RICESTRAW	kg/hr	0.00	0.00	0.00	0.00
ASH	kg/hr	0.00	0.00	0.00	0.00
C	kg/hr	0.00	0.00	0.00	0.00
S	kg/hr	0.00	0.00	0.00	0.00
CH_3COOH	kg/hr	0.00	0.00	0.00	0.00
C_2H_5OH	kg/hr	0.00	0.00	0.00	0.00
		Mass Fractions			
H_2		0.0121	0.0121	0.0000	0.0063
CH_4		0.0020	0.0020	0.0000	0.0021
CO		0.2400	0.2400	0.0000	0.1415
CO_2		0.1263	0.1263	0.0000	0.2004
O_2		0.0000	0.0000	0.2329	0.0104
N_2		0.5737	0.5737	0.7671	0.6391
H_2S		0.0002	0.0002	0.0000	0.0003
H_2O		0.0457	0.0457	0.0000	0.0000
Cl_2		0.0000	0.0000	0.0000	0.0000
RICESTRAW		0.0000	0.0000	0.0000	0.0000
ASH		0.0000	0.0000	0.0000	0.0000
C		0.0000	0.0000	0.0000	0.0000
S		0.0000	0.0000	0.0000	0.0000
CH_3COOH		0.0000	0.0000	0.0000	0.0000
C_2H_5OH		0.0000	0.0000	0.0000	0.0000
Volume Flow	l/min	598253.61	3148905.97	107674.94	2613013.99

https://doi.org/10.24191/mjcet.v7i2.1863

Table B2: Continued

Material		
Stream Name	Units	16
Total Stream		
Temperature	C	30.00
Pressure	bar	0.89
Mass Vapor Fraction		0.00
Mass Liquid Fraction		1.00
Mass Solid Fraction		0.00
Mass Enthalpy	kJ/kg	-10221.09
Mass Density	gm/cc	0.8810
Enthalpy Flow	kW	-48119.48
Mass Flows	kg/hr	16948.31
H_2	kg/hr	0.00
CH_4	kg/hr	0.00
CO	kg/hr	0.00
CO_2	kg/hr	0.00
O_2	kg/hr	0.00
N_2	kg/hr	0.00
H_2S	kg/hr	0.00
H_2O	kg/hr	7087.78
Cl_2	kg/hr	0.00
RICESTRAW	kg/hr	0.00
ASH	kg/hr	0.00
C	kg/hr	0.00
S	kg/hr	0.00
CH_3COOH	kg/hr	776.23
C_2H_5OH	kg/hr	9084.29
Mass Fractions		
H_2		0.0000
CH_4		0.0000
CO		0.0000
CO_2		0.0000
O_2		0.0000
N_2		0.0000
H_2S		0.0000
H_2O		0.4182
Cl_2		0.0000
RICESTRAW		0.0000
ASH		0.0000
C		0.0000
S		0.0000
CH_3COOH		0.0458
C_2H_5OH		0.5360
Volume Flow	l/min	320.64

https://doi.org/10.24191/mjcet.v7i2.1863

Table B3: Meteorological data of the plant

Period	**Air Temperature (°C)**	**Humidity (%)**	**Wind Velocity (m/s)**	**Stability Class**	**Wind Direction**
Day	28	78	2	B	2 wind directions - ENE, SW
Night	28	78	1	F	2 wind directions - ENE, SW

Table B4: Pasquill-Gifford dispersion coefficients for plume dispersion

Pasquill-Gifford stability class	σ_y **(m)**	σ_z **(m)**
Rural conditions		
A	$0.22x(1+0.0001x)^{-0.5}$	$0.20x$
B	$0.16x(1+0.0001x)^{-0.5}$	$0.12x$
C	$0.11x(1+0.0001x)^{-0.5}$	$0.08x(1+0.0002x)^{-0.5}$
D	$0.08x(1+0.0001x)^{-0.5}$	$0.06x(1+0.0015x)^{-0.5}$
E	$0.06x(1+0.0001x)^{-0.5}$	$0.03x(1+0.0003x)^{-1}$
F	$0.04x(1+0.0001x)^{-0.5}$	$0.016x(1+0.0003x)^{-1}$
Urban conditions		
A-B	$0.32x(1+0.0001x)^{-0.5}$	$0.24x(1+0.001x)^{+0.5}$
C	$0.22x(1+0.0001x)^{-0.5}$	$0.20x$
D	$0.16x(1+0.0001x)^{-0.5}$	$0.14x(1+0.0003x)^{-0.5}$
E-F	$0.11x(1+0.0001x)^{-0.5}$	$0.08x(1+0.0015x)^{-0.5}$

Table B5: Pasquill-Gifford dispersion coefficients for puff dispersion

Pasquill-Gifford stability class	σ_y **(m) or** σ_x **(m)**	σ_z **(m)**
A	$0.18x^{0.92}$	$0.60x^{0.75}$
B	$0.14x^{0.92}$	$0.53x^{0.73}$
C	$0.10x^{0.92}$	$0.34x^{0.71}$
D	$0.06x^{0.92}$	$0.15x^{0.70}$
E	$0.04x^{0.92}$	$0.10x^{0.65}$
F	$0.02x^{0.89}$	$0.05x^{0.61}$

https://doi.org/10.24191/mjcet.v7i2.1863